

Numerical Solution of Fractional order Chlamydia Model Via the Generalized Fractional Adams-Bashforth-Moulton Approach

³Joseph Egbemhenghe, ⁴Lebechi Faith Akor, ^{1,2}*William Atokolo, ^{1,2}Jeremiah Amos

¹Department of Mathematical Sciences, Prince Abubakar Audu University, Anyigba, Nigeria

²Laboratory of Mathematical Epidemiology, Prince Abubakar Audu University, Anyigba.

³Department of Mathematics Education, Prince Abubakar Audu University, Anyigba
(Formerly known as Kogi State University Anyigba), Nigeria.

⁴Department of Mathematics, Federal University of Technology Owerri, Imo State, Nigeria

**Corresponding author: williamsatokolo@gmail.com*

Abstract

In this study we examine the epidemiological features of chlamydia infection using a fractional-order mathematical model, evaluating the impact of vaccine and therapy on the dynamics of disease transmission. In the fractional-order framework, the study determines the existence and uniqueness of solutions and uses the Lyapunov function approach to examine the stability of the endemic equilibrium. Numerical simulations that employ the fractional Adams–Bashforth–Moulton approach show how fractional-order values and model parameters impact the control and spread of the disease. More simulations, such as surface and contour plots, show that a higher prevalence of chlamydia is a result of increased contact rates and decreased treatment effectiveness. The results highlight how the infection's spread within the community can be successfully stopped by improving vaccine and treatment plans.

Keywords and phrases: Chlamydia, Fractional, Adam-Bashforth-Moulton, Transmission, Control, strategies.

1.0 Introduction

Chlamydia trachomatis is the most prevalent sexually transmitted infection (STI) globally [1], with an estimated 129 million cases reported in 2020 [1][2]. This bacterial infection is primarily transmitted through sexual contact, including vaginal, anal, and oral sex with an infected individual. Non-sexual transmission can also occur via direct hand-to-hand contact, sharing clothes, bedding, or towels, or through flies exposed to infectious nasal or eye secretions. In rare cases, the infection can lead to conjunctivitis. Importantly, Chlamydia trachomatis is a major global cause of blindness [3].

How to cite: Egbemhenghe, J., Faith Akor, L., Atokolo, W., & Amos, J. (2025). Numerical Solution of Fractional order Chlamydia Model Via the Generalized Fractional Adams-Bashforth-Moulton Approach. *GPH - International Journal of Mathematics*, 8(01), 01-23. <https://doi.org/10.5281/zenodo.14716850>



This work is licensed under Creative Commons Attribution 4.0 License.

The infection affects both genders but is more common in women, with prevalence rates of 4.2% in females and 2.7% in males [4,5]. Adolescents and young adults, particularly sexually active women aged 15 to 24, are at the highest risk [6]. In women, the infection can harm the throat, rectum, and cervix, often resulting in pelvic inflammatory disease (PID), infertility, ectopic pregnancies, or miscarriages [7,8]. It can also be transmitted from an infected mother to her newborn during vaginal delivery [6]. Symptoms in women may include unpleasant-smelling vaginal discharge, itching, burning, bleeding, abdominal pain, and fever. Men may experience painful urination, swollen testicles, and penile discharge. The incubation period typically ranges from 7 to 20 days. While Chlamydia infections are treatable with antibiotics such as azithromycin or doxycycline, abstaining from sexual activity during treatment is crucial to prevent further transmission. However, re-infection is possible even after successful treatment [9].

Mathematical modeling plays a crucial role in understanding the transmission dynamics of infectious diseases such as Chlamydia. These models help identify the key factors driving epidemics and assist in developing effective control strategies. While conventional models have been extensively utilized, they often fail to account for memory effects or the long-term dependencies characteristic of biological processes. To address this limitation, fractional-order models have emerged as a valuable alternative. These models incorporate non-local properties, enabling the inclusion of memory effects and anomalous diffusion in the study of disease transmission [10].

Fractional differential equations (FDEs) extend traditional integer-order models, offering a more versatile framework for modeling complex systems. This research introduces a fractional-order mathematical model to describe the transmission dynamics of Chlamydia, incorporating treatment and prevention measures as control strategies. By leveraging the memory effect characteristic of fractional calculus, the model provides a more accurate representation of the disease's spread. Through simulations of various intervention scenarios, the study seeks to determine the most effective methods for reducing Chlamydia prevalence and ensuring sustainable infection control.

Fractional derivatives, which capture memory and hereditary characteristics in biological systems, provide significant advantages in modeling diseases such as Chlamydia. They allow for a more comprehensive analysis of infection progression over time and the impact of individuals' infection and treatment histories on transmission dynamics. This nuanced approach supports the design of more realistic and effective control strategies, tackling enduring issues like drug resistance, re-infection, and constraints in healthcare resources.

Recent advancements in fractional calculus, as emphasized by Atokolo et al. [11], have highlighted its effectiveness in describing the dynamic behavior of various systems. Unlike classical integer-order models that primarily address local properties, fractional-order models capture global system behavior, including memory effects. These models are not only more realistic but also better suited for real-world applications, making them invaluable for understanding and controlling the spread of infectious diseases like Chlamydia.

In biological contexts, fractional derivatives such as the Caputo and Riemann-Liouville derivatives, which have singular kernels, are widely used. Non-singular kernel derivatives,

such as the Mittag-Leffler and Atangana-Baleanu operators, have also gained popularity for their enhanced applicability.

Atokolo et al. [11] proposed a fractional-order Sterile Insect Technology (SIT) model for controlling Zika virus transmission, employing the LADM technique to derive infinite series solutions converging to exact values. Similarly, Atokolo et al. [12] analyzed Lassa fever dynamics using a fractional-order model with a power-law derivative to examine the impacts of vaccination and treatment on disease spread.

Other notable studies include Yunus et al. [13], who used a Caputo fractional-order derivative to model COVID-19 control in Nigeria, revealing higher recovery rates under integer-order scenarios due to vaccination and treatment. Omede et al. [14] developed a Caputo-based fractional-order compartmental model for soil-transmitted helminth infections, demonstrating greater solution flexibility using LADM.

Amos et al. [15] created a fractional model for hepatitis C transmission, utilizing the Adams-Bashforth-Moulton method to show that reducing contact rates and improving treatment significantly curtailed disease spread. James et al. [16] and Abah et al. [17] employed similar fractional approaches for studying HIV/AIDS and Diphtheria, respectively, showcasing the superior adaptability of fractional models compared to classical methods.

Additionally, Ahmed et al. [18] developed an ABC-fractional order model for HIV and COVID-19 co-epidemic dynamics, while Smith et al. [19] reviewed the co-infection dynamics of hepatitis C and COVID-19, identifying key methods and research gaps. Ullah et al. [20], as cited by Das et al. [21], applied a hybrid Laplace transform and Adomian Decomposition Method to address fuzzy Volterra integral equations, advancing the theoretical framework of fuzzy analytical dynamic equations.

The advantages of fractional-order models lie in their flexibility and ability to capture non-local effects. Unlike classical derivatives, fractional derivatives more accurately approximate real-world phenomena, account for memory effects, and incorporate non-local interactions—features often absent in integer-order models. These properties make fractional differential equations a powerful tool for addressing complex problems in infectious disease modeling and beyond.

Ali et al. [22] investigated the stability and existence of solutions for a three-point boundary value problem, focusing on various types of Ulam stability. Their study utilized classical nonlinear fractional methods to analyze the problem, offering significant contributions to the field.

The primary objectives of this paper are as follows:

- Establish conditions that guarantee the existence and uniqueness of solutions for the proposed fractional-order model.
- Conduct a stability analysis of the endemic equilibrium point using the Lyapunov function method.

- Obtain numerical solutions through the fractional Adams–Bashforth–Moulton method.
- Perform numerical simulations to assess the model's behavior.

A review of existing literature on mathematical models and transmission dynamics of Chlamydia highlights a gap in studies employing fractional calculus alongside the Adams–Bashforth–Moulton method to simulate and analyze Chlamydia transmission and control strategies.

The structure of this paper is as follows: Section 2 presents the formulation of the mathematical model, Section 3 focuses on its analytical properties, Section 4 showcases numerical results for the fractional-order model, and Section 5 concludes with a summary and key observation.

1.1 Preliminary

This section offers an overview of essential concepts and fundamental results from fractional calculus. The analysis utilizes both right and left fractional Caputo derivatives, adhering to the frameworks proposed by [23,24]. Furthermore, the discussion underscores the practical applications of fractional calculus in solving real-world problems across diverse fields such as physics, engineering, biomathematics, and other scientific disciplines.

Definition 1: Let $f \in \Lambda^\infty(R)$ then the left and right Caputo fractional derivative of the function f is given by

$${}^c D_t^\sigma f(t) = \left(t^0 D_t^{-(n-\sigma)} \left(\frac{d}{dt} \right)^n f(t) \right)$$

$${}^c D_t^\sigma f(t) = \frac{1}{\Gamma(n-\sigma)} \int_0^t (t-\lambda)^{n-\sigma-1} f^n(\lambda) d\lambda \quad (1)$$

The same way

$${}^c D_t^\sigma f(t) = \left(D_T^{-(n-\sigma)} \left(\frac{-d}{dt} \right)^n \right) f(t)$$

$${}^c D_T^\sigma f(t) = \frac{(-1)^n}{\Gamma(n-\sigma)} \int_t^T (\lambda-t)^{n-\sigma-1} f^n(\lambda) d\lambda$$

Definition 2: The generalized Mittag-Leffler function $E_{\alpha,\beta}(x)$ for $x \in R$ is given by

$$E_{\alpha,\beta}(x) = \sum_{n=0}^{\infty} \frac{x^n}{\Gamma(\alpha n + \beta)}, \quad \alpha, \beta > 0 \quad (2)$$

which can also be represented as

$$E_{\alpha,\psi}(x) = xE_{\alpha,\alpha+\psi(x)} + \frac{1}{\Gamma(\psi)} \quad (3)$$

$$E_{\alpha,\psi}(x) = L \left[t^{\psi-1} E_{\alpha,\psi(\pm \omega t^\alpha)} \right] = \frac{S^{\alpha-\psi}}{S^\alpha \pm \omega} \quad (4)$$

Proposition 1.1.

Let $f \in \Lambda^\infty(R) \cap C(R)$ and $\alpha \in R, n-1 < \alpha < n$,

therefore, the conditions given below holds:

1. ${}^C D_t^\sigma I^\sigma f(t) = f(t)$
2. ${}^C D_t^\sigma I^\sigma f(t) = f(t) - \sum_{k=0}^{n-k} \frac{t^k}{K!} f^{(k)}(t_0)$

2.0 Model Formulation and Description

The rate at which individuals are added to the susceptible population is represented as π , so that β_1, β_2 is the effective contact rate between the susceptible and infected humans and individuals on Chlamydia treatment respectively. We represent θ as the rates at which individuals move from the exposed Chlamydia classes to the infected class. The rate of treatment for infected individuals with Chlamydia is represented as α and σ denotes the recovery rate of treated humans due to Chlamydia. The natural death rate of humans is denoted as μ . The disease induced death rate of infected humans with Chlamydia and humans on Chlamydia treatment, is denoted as δ_1, δ_2 . The vaccination rate of susceptible humans against Chlamydia is denoted as ω_2 and the rate of vaccine failure is denoted as ω_1 .

2.1 Model Assumptions

1. We assumed an imperfect vaccine that is there is possibility of vaccine failure.
2. We assume that recovered humans from Chlamydia can become susceptible to it even after recovery from the disease.
3. We assumed that individuals infected with Chlamydia get full recovery from the disease in the treatment class.

2.2 Schematic Diagram of The Chlamydia Model

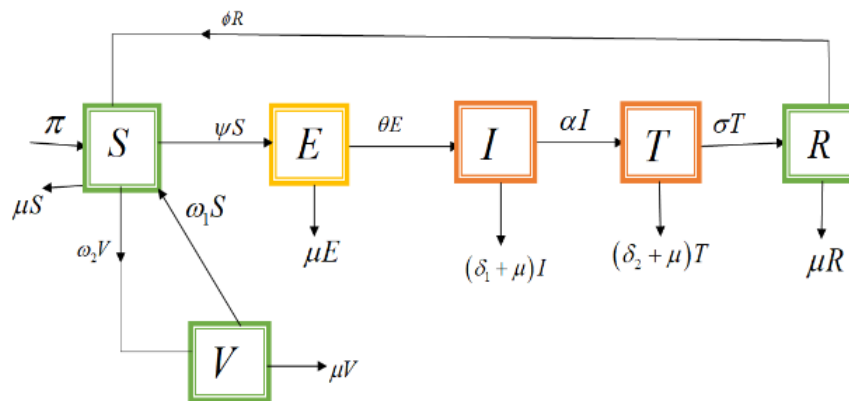


Fig.1: Chlamydia Model Flow Diagram

2.3 Model Equation

The differential equations modeling the transmission dynamics of Chlamydia in the human population is given as:

$$\begin{aligned}
 \frac{dS}{dt} &= \pi + \omega_1 V + \phi R - (\lambda + \omega_2 + \mu) S, \\
 \frac{dE}{dt} &= \psi S - (\theta + \mu) E, \\
 \frac{dV}{dt} &= \omega_2 S - (\omega_1 + \mu) V, \\
 \frac{dI}{dt} &= \theta E - (\alpha + \delta_1 + \mu) I, \\
 \frac{dT}{dt} &= \alpha I - (\sigma + \delta_2 + \mu) T, \\
 \frac{dR}{dt} &= \sigma T - \mu R.
 \end{aligned} \tag{5}$$

Where $\psi = \frac{(\beta_1 I + \beta_2 T)}{N}$

2.4 Table of Model Variables and Parameters

VARIABLE	DESCRIPTION
$S(t)$	Population of Susceptible Humans
$V(t)$	Vaccinated Human population
$E(t)$	Exposed Humans to Chlamydia
$I(t)$	Infected Humans with Chlamydia
$T(t)$	Humans on Chlamydia treatment

$R(t)$	Recovered humans from Chlamydia
Parameters	Descriptions
π	Recruitment rate
β_1	The effective contact rate between the susceptible and infected humans
β_2	The effective contact rate between the susceptible individuals and humans on Chlamydia treatment
θ	The progression rates from exposed Chlamydia classes to infected class
α	Treatment rate of humans with Chlamydia.
σ	Recovery due to treatment rate
μ	Natural death rate
δ_1	The mortality rate of infected individuals caused by the disease
δ_2	The mortality rate of humans on Chlamydia treatment
ϕ	Rate at which recovered humans becomes susceptible again
ω_1	Waning rate
ω_2	Vaccination rate

3.0 Fractional Chlamydia mathematical model

In this section, the integer-order Chlamydia model from Eq. (5) is extended by incorporating the Caputo fractional derivative operator. This modification offers greater flexibility compared to the traditional model in Eq. (5), as the fractional-order approach allows for a wider spectrum of dynamic behaviors. The resulting fractional-order Chlamydia model is presented as follows: ${}^C D_t^\sigma S = \pi + \omega_1 V + \phi R - (\psi + \omega_2 + \mu) S$,

$${}^C D_t^\sigma E = \psi S - (\theta + \mu) E,$$

$${}^C D_t^\sigma V = \omega_2 S - (\omega_1 + \mu) V,$$

$${}^C D_t^\sigma I = \theta E - (\alpha + \delta_1 + \mu) I, \quad (6)$$

$${}^C D_t^\sigma T = \alpha I - (\sigma + \delta_2 + \mu) T,$$

$${}^C D_t^\sigma R = \sigma T - \mu R.$$

Subject to the positive initial conditions

$$S(0) = S_0, E(0) = E_0, V(0) = V_0, I(0) = I_0, T(0) = T_0, R(0) = R_0. \quad (7).$$

3.1 Positivity of model solution

We considered the non-negativity of the initial values

$$\limsup N(t) \leq \frac{\pi}{\mu},$$

Secondly, if $\limsup N_0(t) \leq \frac{\pi}{\mu}$, the feasible domain of our model is defined as:

$$\Omega = \left\{ (S, E, V, I, T, R) \in R_+^6 : S + E + V + I + T + R \leq \frac{\pi}{\mu} \right\}, \text{ so that}$$

$$\Omega = \Omega_c \subset R_+^6,$$

hence, Ω is positively invariant.

If $S_0, E_0, V_0, I_0, T_0, R_0$ are non-negative, then the solution of model (6) remains non-negative for $t > 0$. From Eq. (6), considering the first equation, we obtain

$${}^c D_t^\sigma S = \pi + \omega_1 V + \phi R - (\psi + \omega_2 + \mu) S,$$

$${}^c D_t^\sigma S + (\psi + \omega_2 + \mu) S = \pi + \omega_1 V + \phi R,$$

But $\pi + \omega_1 V + \phi R \geq 0$ then,

$${}^c D_t^\sigma S + (\psi + \omega_2 + \mu) S \geq 0 \tag{8}$$

Applying the Laplace transform we obtained;

$$L[{}^c D_t^\sigma S] + L[(\psi + \omega_2 + \mu) S] \geq 0$$

$$S^\sigma S(s) - S^{\sigma-1} S(0) + (\psi + \omega_2 + \mu) S(s) \geq 0,$$

$$S(s) \geq \frac{S^{\sigma-1}}{S^\sigma + (\psi + \omega_2 + \mu)} S(0),$$

By taking the inverse Laplace transforms, we obtained;

$$S(t) \geq E_{\sigma,1}(-(\lambda + \omega_2 + \mu)t^\sigma) S_0, \tag{9}$$

Since the term on the right-hand side of Eq. (9) is positive, it follows that for $t > 0$. In similar way, we say that $S \geq 0, E \geq 0, V \geq 0, I \geq 0, T \geq 0, R \geq 0$. that is are positives, consequently, the solution will remain in R_+^6 for all $t > 0$ with positive initial situation.

3.2 Boundedness of fractional model solution

The total population of individuals from our model is given by;

$$N(t) = S(t) + E(t) + V(t) + I(t) + T(t) + R(t).$$

So from our fractional model (6), we now obtain

$${}^c D_t^\sigma N(t) = {}^c D_t^\sigma S(t) + {}^c D_t^\sigma E(t) + {}^c D_t^\sigma V(t) + {}^c D_t^\sigma I(t) + {}^c D_t^\sigma T(t) + {}^c D_t^\sigma R(t).$$

$${}^c D_t^\sigma N(t) \leq \pi - \mu N(t) \quad (10)$$

Taking the Laplace transformation of (10) we now have;

$$L[{}^c D_t^\sigma N(t)] \leq L[\pi - \mu N(t)],$$

$$S^\sigma N(s) - S^{\sigma-1} N(0) + \mu N(s) \leq \frac{\pi}{\mu},$$

$$N(s) \leq \frac{S^{\sigma-1}}{(S^\sigma + \mu)} N(0) + \frac{\pi}{S(S^\sigma + \mu)}, \quad (11)$$

Taking the inverse Laplace transform of Eq. (11) we have ;

$$N(t) \leq E_{\sigma,1}(-\mu t^\sigma) N(0) + \pi E_{\sigma,\sigma+1}(-\mu t^\sigma), \quad (12)$$

At $t \rightarrow \infty$, the limit of Eq. (12) becomes

$$\lim_{t \rightarrow \infty} \text{Sup} N(t) = \frac{\pi}{\mu}.$$

This means that, if $N_0 \leq \frac{\pi}{\mu}$ then $N \leq \frac{\pi}{\mu}$ which implies that, $N(t)$ is enclosed or bounded.

We now conclude that, this region $\Omega = \Omega_H$, is well posed and similarly feasible epidemiologically.

3.3 Existence and uniqueness of our model solution

Let the real, non-negative value be H , we $Q = [0, H]$.

The set of all continuous function that is defined on M is represented by $N_e^0(Q)$ with norm as;

$$\|X\| = \text{Sup}\{X(t), t \in Q\} \quad (13)$$

Considering model (6) with initial conditions presented in (8) which can be denoted as an initial value problem (IVP) in (13).

$${}^c D_t^\sigma(t) = Z(t, X(t)), 0 < t < H < \infty,$$

$$X(0) = X_0.$$

Where $Y(t) = (S(t), E(t), V(t), I(t), T(t), R(t))$ represents the groups and Z be a continuous function defined as follows;

$$= \begin{pmatrix} \pi + \omega_1 V + \phi R - \left(\frac{(\beta_1 I + \beta_2 T)}{N} + \omega_2 + \mu \right) S \\ \frac{(\beta_1 I + \beta_2 T)}{N} S - (\theta + \mu) E \\ \omega_2 S - (\omega_1 + \mu) V \\ \theta E - (\alpha + \delta_1 + \mu) I \\ \alpha I - (\sigma + \delta_2 + \mu) T \\ \sigma T - \mu R \end{pmatrix} \quad (14)$$

Using proposition (2.1), we have that,

$$\begin{aligned} S(t) &= S_0 + I_t^\sigma \left[\pi + \omega_1 V + \phi R - \left(\frac{(\beta_1 I + \beta_2 T)}{N} + \omega_2 + \mu \right) S \right], \\ E(t) &= E_0 + I_t^\sigma \left[\frac{(\beta_1 I + \beta_2 T)}{N} S - (\theta + \mu) E \right], \\ V(t) &= V_0 + I_t^\sigma \left[\omega_2 S - (\omega_1 + \mu) V \right], \\ I(t) &= I_0 + I_t^\sigma \left[\theta E - (\alpha + \delta_1 + \mu) I \right], \\ T(t) &= T_0 + I_t^\sigma \left[\alpha I - (\sigma + \delta_2 + \mu) T \right], \\ R(t) &= R_0 + I_t^\sigma \left[\sigma T - \mu R \right]. \end{aligned} \quad (15)$$

We have the Picard iteration of (15) as follows;

$$\begin{aligned} S(t) &= S_0 + \frac{1}{\Gamma(\sigma)} \int_0^t (t-\lambda)^{\sigma-1} Z_1(\lambda, S_{(n-1)}(\lambda)) d\lambda, \\ E(t) &= E_0 + \frac{1}{\Gamma(\sigma)} \int_0^t (t-\lambda)^{\sigma-1} Z_2(\lambda, E_{(n-1)}(\lambda)) d\lambda, \\ V(t) &= V_0 + \frac{1}{\Gamma(\sigma)} \int_0^t (t-\lambda)^{\sigma-1} Z_3(\lambda, V_{(n-1)}(\lambda)) d\lambda, \\ I(t) &= I_0 + \frac{1}{\Gamma(\sigma)} \int_0^t (t-\lambda)^{\sigma-1} Z_4(\lambda, I_{(n-1)}(\lambda)) d\lambda, \\ T(t) &= T_0 + \frac{1}{\Gamma(\sigma)} \int_0^t (t-\lambda)^{\sigma-1} Z_5(\lambda, T_{(n-1)}(\lambda)) d\lambda, \\ R(t) &= R_0 + \frac{1}{\Gamma(\sigma)} \int_0^t (t-\lambda)^{\sigma-1} Z_6(\lambda, R_{(n-1)}(\lambda)) d\lambda. \end{aligned} \quad (16)$$

We now transformed the initial value problem of Eq. (13) to obtain;

$$X(t) = X(0) + \frac{1}{\Gamma(\sigma)} \int_0^t (t-\lambda)^{\sigma-1} Z(\lambda, X(\lambda)) d\lambda. \quad (17)$$

Lemma 1, The Lipchitz condition described from Eq. (14) is satisfied by vector $Z(t, X(\lambda))$ on a set $[0, H] \times R_+^6$ with the Lipchitz constant given as;

$$\eta = \max\left((\beta_1^* + \beta_2^* + \omega_2 + \mu), (\theta + \mu), (\omega_1 + \mu), (\alpha + \delta_1 + \mu), (\sigma + \delta_2 + \mu), (\mu)\right).$$

Proof.

$$\begin{aligned} & \|Z_1(t, S) - Z_1(t, S_1)\| \\ &= \left\| \pi + \omega_1 V + \phi R - \left(\frac{(\beta_1 I + \beta_2 T)}{N} + \omega_2 + \mu \right) S - \pi - \omega_1 V - \phi R - \left(\frac{(\beta_1 I + \beta_2 T)}{N} + \omega_2 + \mu \right) S_1 \right\| \\ &= \left\| - \left(\frac{(\beta_1 I + \beta_2 T)}{N} + \omega_2 + \mu \right) (S - S_1) + \mu (S - S_1) \right\| \leq \left((\beta_1^* + \beta_2^*) \right) \|S - S_1\| + \|\mu(S - S_1)\| \\ &\therefore \|Z_1(t, S) - Z_1(t, S_1)\| \leq \left((\beta_1^* + \beta_2^*) + \omega_2 + \mu \right) \|S - S_1\| + \|\mu(S - S_1)\| \end{aligned}$$

Similarly we obtained the following;

$$\begin{aligned} & \|Z_2(t, E) - Z_2(t, E_1)\| \leq (\theta + \mu) \|E - E_1\|, \\ & \|Z_3(t, V) - Z_3(t, V_1)\| \leq (\omega_1 + \mu) \|V - V_1\|, \quad (18) \\ & \|Z_4(t, I) - Z_4(t, I_1)\| \leq (\alpha + \delta_1 + \mu) \|I - I_1\|, \\ & \|Z_5(t, T) - Z_5(t, T_1)\| \leq (\sigma + \delta_2 + \mu) \|T - T_1\|, \\ & \|Z_6(t, R) - Z_6(t, R_1)\| \leq (\mu) \|R - R_1\|. \end{aligned}$$

Where we obtained

$$\begin{aligned} & \|Z_1(t, X_1(t)) - Z_1(t, X_2(t))\| \leq \beta \|X_1 - X_2\|, \\ & \eta = \max\left((\beta_1^* + \beta_2^* + \omega_2 + \mu), (\theta + \mu), (\omega_1 + \mu), (\alpha + \delta_1 + \mu), (\sigma + \delta_2 + \mu), (\mu)\right). \quad (19) \end{aligned}$$

Lemma 2. The initial value problem defined by (6) and (7) in Eq. (19) has a unique solution and exists.

$$X(t) \in A_c^0(f).$$

Using Picard-Lindelof and fixed-point theory, we estimate the solution of

$$X(t) = S(X(t)),$$

we defined S as the Picard operator articulated as;

$$S : A_c^0(f, R_+^6) \rightarrow A_c^0(f, R_+^6)$$

Therefore

$$S(X(t)) = X(0) + \frac{1}{\Gamma(\sigma)} \int_0^t (t-\lambda)^{\sigma-1} Z_1(\lambda, X(\lambda)) d\lambda, \quad (20)$$

which becomes

$$\begin{aligned} & \|S(X_1(t)) - S(X_2(t))\| \\ &= \frac{1}{\Gamma(\sigma)} \left[\int_0^t (t-\lambda)^{\sigma-1} Z(\lambda, X_1(\lambda)) - Z(\lambda, X_2(\lambda)) d\lambda \right], \\ &\leq \frac{1}{\Gamma(\sigma)} \left[\int_0^t (t-\lambda)^{\sigma-1} Z(\lambda, X_1(\lambda)) - Z(\lambda, X_2(\lambda)) d\lambda \right], \\ &\leq \frac{\eta}{\Gamma(\sigma)} \left[\int_0^t (t-\lambda)^{\sigma-1} \|X_1 - X_2\| d\lambda \right], \\ &\|S(X_1(t)) - S(X_2(t))\| \leq \frac{\eta}{\Gamma(\sigma+1)} S. \end{aligned} \quad (21)$$

When, $\frac{\eta}{\Gamma(\sigma+1)} S \leq 1$, then the Picard operator provides a contradiction, ensuring that the solution to Eq. (6) and (7) is unique.

3.4 The basic reproduction number (R_0) and model equilibrium points:

The disease-free equilibrium points of model (5) are represented as:

$$\varepsilon_0 = (S^0, E^0, V^0, I^0, T, R^0) = \left(\frac{(\omega_1 + \mu)\pi}{\mu(\mu + \omega_2 + \omega_1)}, 0, \frac{\omega_2\pi}{\mu(\mu + \omega_2 + \omega_1)}, 0, 0, 0 \right). \quad (22)$$

To calculate the basic reproduction number, we use the next-generation method.

$$n = (E, I, T)$$

Let

$$\frac{dn}{dt} = FV^{-1}$$

So that,

Where,

$$F = \begin{bmatrix} 0 & \frac{\beta_1(\omega_1 + \mu)}{\omega_1 + \theta + \mu_h} & \frac{\beta_2(\omega_1 + \mu)}{\omega_1 + \theta + \mu_h} \\ 0 & 0 & 0 \\ 0 & 0 & 0 \end{bmatrix}$$

$$V = \begin{bmatrix} A_1 & 0 & 0 \\ -\theta & A_2 & 0 \\ 0 & -\alpha & A_3 \end{bmatrix}$$

$$R_0 = \frac{\theta(\alpha\mu\beta_2 + \alpha\beta_2\omega_1 + \mu A_3\beta_1 + A_3\beta_1\omega_1)}{(\mu + \omega_2 + \omega_1)A_1A_2A_3}. \quad (23)$$

Where $A_1 = (\theta + \mu)$, $A_2 = (\alpha + \delta_1 + \mu)$, $A_3 = (\sigma + \delta_2 + \mu)$.

3.5 Endemic Equilibrium point

We explored the potential for an endemic equilibrium point, representing a stable state where Chlamydia continues to exist within the population. At this equilibrium, the model's variables stay positive and maintain non-zero values.

$(S^* \neq 0, E^* \neq 0, V^* \neq 0, I^* \neq 0, T^* \neq 0, R^* \neq 0)$.

To investigate the endemic equilibrium point, the model equations are restructured according to the infection rates within the populations. Using the fractional Chlamydia model (6), the endemic equilibrium state is defined as follows:

$$S^* = \frac{\pi\mu P_2 P_3 P_4 P_5}{\mu P_2 P_4 P_5 (P_1 P_3 - \omega_1 \omega_2) - \alpha\phi\psi\sigma\theta P_3},$$

$$E^* = \frac{\pi\mu P_3 P_4 P_5 \psi}{\mu P_2 P_4 P_5 (P_1 P_3 - \omega_1 \omega_2) - \alpha\phi\psi\sigma\theta P_3},$$

$$V^* = \frac{\pi\mu P_2 P_4 P_5 \omega_2}{\mu P_2 P_4 P_5 (P_1 P_3 - \omega_1 \omega_2) - \alpha\phi\psi\sigma\theta P_3}, \quad (24)$$

$$I^* = \frac{\theta P_3 \pi \mu P_5 \psi}{\mu P_2 P_4 P_5 (P_1 P_3 - \omega_1 \omega_2) - \alpha\phi\psi\sigma\theta P_3},$$

$$T^* = \frac{\theta P_3 \pi \mu \psi \alpha}{\mu P_2 P_4 P_5 (P_1 P_3 - \omega_1 \omega_2) - \alpha\phi\psi\sigma\theta P_3},$$

$$R^* = -\frac{\theta P_3 \pi \psi \alpha \sigma}{\alpha\phi\psi\sigma\theta P_3 - \mu P_1 P_2 P_3 P_4 P_5 + \mu P_2 P_4 P_5 \omega_1 \omega_2}.$$

Substituting into the force of infection $\psi = \frac{(\beta_1 I + \beta_2 T)}{N}$

$$B_1 = (\alpha \mu \psi \theta P_3 + \psi \alpha \sigma \theta P_3 + \mu \psi \theta P_3 P_5 + \mu \psi P_3 P_4 P_5 + \mu P_2 P_3 P_4 P_5 + \mu P_2 P_4 P_5 \omega_2),$$

$$B_2 = \mu \psi \theta P_3 (1 - R_0). \quad (25)$$

Where, $P_1 = (\omega_2 + \mu)$, $P_2 = (\theta + \mu)$, $P_3 = (\omega_1 + \mu)$, $P_4 = (\alpha + \delta_1 + \mu)$, $P_5 = (\sigma + \delta_2 + \mu)$, $P_6 = (\mu)$.

This implies that the model has a stable endemic equilibrium point.

3.6 Global Stability of Chlamydia Disease

Theorem 1: Prove that the system (5) is globally asymptotically stable at Disease free equilibrium, moreover, at $R_0 < 1$.

Proof

We develop the Lyapunov function to validate the results.

$$L = u_1 (S - S_0) + u_2 (E - E_0) + u_3 (V - V_0) + u_4 (I - I_0) + u_5 (T - T_0) + u_6 (R - R_0). \quad (26)$$

Where $u_1, u_2, u_3, u_4, u_5, u_6$ are positive constants.

Taking the derivative of a Lyapunov function, we obtained;

$$L' = \pi u_1 + \omega_1 S E (u_2 - u_1) + (1 - \omega_2) (u_3 - u_1) + \alpha (u_3 - u_2) + \omega_2 (u_4 - u_2) + \theta_1 (u_4 - u_3) \\ + \omega_2 (u_5 - u_4) + \alpha (u_6 - u_4) - \mu u_1 S - \mu u_2 E - \mu u_3 V - \mu u_4 I - \mu u_5 T - \mu u_6 R.$$

Choosing the positive constants $u_1 = u_2 = u_3 = u_4 = u_5 = u_6 = 1$

And $N > \frac{\pi}{\mu}$ then, we obtained;

$$L' = \pi - \mu N$$

$$L' = -[\mu N - \pi] < 0. \quad (27)$$

Hence the system (5) is globally asymptotically stable at the Disease-free equilibrium and at $R_0 < 1$.

3.7 Fractional order model numerical results

We numerically solved the fractional-order Chlamydia model using the generalized fractional Adams-Bashforth-Moulton method outlined in [24]. The parameter values applied in the model are listed in Table 1, which also presents various fractional order values. (σ) are considered and simulated.

3.8 Implementation of fractional Adams–Bashforth–Moulton method

The approach outlined by [25, 9] has been utilized in this study. By employing the fractional Adams-Bashforth-Moulton method, we obtained an approximate solution for the fractional Chlamydia model given in equation (6). The fractional model (6) is now

$${}^c D_t^\sigma H(t) = Q(t, q(t)), \quad 0 < t < \eta, \quad (28)$$

$$H^{(n)}(0) = H_0^{(n)}, \quad n = 1, 0, \dots, q, q = [\alpha].$$

Where $H = (S^*, E^*, V^*, I^*, T^*, R^*) \in R_+^6$ and $V(t, q(t))$ is a real valued function that is continuous.

Eq. (27) can thus be expressed using the concept of fractional integral as follows:

$$H(t) = \sum_{n=0}^{m-1} H_0^{(n)} \frac{t^n}{n!} + \frac{1}{\Gamma(\sigma)} \int_0^t (t-y)^{\sigma-1} R(k, m(k)) dk \quad (29)$$

Using the method described in [43], we let the step size $g = \frac{\eta}{N}$, $N \in \mathbb{N}$ with a grid that is uniform on $[0, \eta]$. Where $t_c = cr$, $c = 0, 1, \dots, N$. Hence, the fractional-order Chlamydia model presented in (6) can be approximated as:

$$\begin{aligned} S_{k+1}(t) &= S_0 + \frac{g^\sigma}{\Gamma(\sigma+2)} \left\{ \frac{dS}{dt} = \pi + \omega_1 V + \phi R - \frac{(\beta_1 I^n + \beta_1 T^n) S}{N} - P_1 S \right\} + \\ &\frac{g^\sigma}{\Gamma(\sigma+2)} \sum_{y=0}^k dy, k+1 \left\{ \pi + \omega_1 V + \phi R - \frac{(\beta_1 I_y + \beta_1 T_y) S_y}{N_y} - P_1 S_y \right\}, \\ E_{k+1}(t) &= E_0 + \frac{g^\sigma}{\Gamma(\sigma+2)} \left\{ (\beta_1 I^n + \beta_2 T^n) \frac{S^n}{N^n} - P_2 E^n \right\} + \\ &\frac{g^\sigma}{\Gamma(\sigma+2)} \sum_{y=0}^k dy, k+1 \left\{ (\beta_1 I_y + \beta_2 T_y) \frac{S_y}{N_y} - P_2 E_y \right\}, \end{aligned} \quad (30)$$

$$\begin{aligned} V_{k+1}(t) &= V_0 + \frac{g^\sigma}{\Gamma(\sigma+2)} \left\{ \omega_2 S^n - P_3 V^n \right\} + \\ &\frac{g^\sigma}{\Gamma(\sigma+2)} \sum_{y=0}^k dy, k+1 \left\{ \omega_2 S_y - P_3 V_y \right\}, \\ I_{k+1}(t) &= I_0 + \frac{g^\sigma}{\Gamma(\sigma+2)} \left\{ \theta E^n - P_4 I^n \right\} + \\ &\frac{g^\sigma}{\Gamma(\sigma+2)} \sum_{y=0}^k dy, k+1 \left\{ \theta E_y - P_4 I_y \right\}, \end{aligned}$$

$$T_{k+1}(t) = T_0 + \frac{g^\sigma}{\Gamma(\sigma+2)} \{ \alpha I^n - P_5 T^n \} +$$

$$\frac{g^\sigma}{\Gamma(\sigma+2)} \sum_{y=0}^k dy, k+1 \{ \alpha I_y - P_5 T_y \},$$

$$R_{k+1}(t) = T_0 + \frac{g^\sigma}{\Gamma(\sigma+2)} \{ \sigma T^n - \mu R^n \} +$$

$$\frac{g^\sigma}{\Gamma(\sigma+2)} \sum_{y=0}^k dy, k+1 \{ \sigma T_y - \mu R_y \}.$$

Where

$$S_{k+1}^n(t) = S_0 + \frac{1}{\Gamma(\sigma)} \sum_{y=0}^k f_{y,k+1} \left\{ \pi + \omega_1 V + \phi R - (\beta_1 I_y + \beta_1 T_y) \frac{S_y}{N_y} - P_1 S_y \right\},$$

$$E_{k+1}^n(t) = E_0 + \frac{1}{\Gamma(\sigma)} \sum_{y=0}^k f_{y,k+1} \left\{ (\beta_1 I_y + \beta_2 T_y) \frac{S_y}{N_y} - P_2 E_y \right\} \quad (31)$$

$$V_{k+1}^n(t) = V_0 + \frac{1}{\Gamma(\sigma)} \sum_{y=0}^k f_{y,k+1} \{ \omega_2 S - P_3 V \}$$

$$I_{k+1}^n(t) = I_0 + \frac{1}{\Gamma(\sigma)} \sum_{y=0}^k f_{y,k+1} \{ \theta E - P_4 I \},$$

$$T_{k+1}^n(t) = T_0 + \frac{1}{\Gamma(\sigma)} \sum_{y=0}^k f_{y,k+1} \{ \alpha I - P_5 T \},$$

$$R_{k+1}^n(t) = R_0 + \frac{1}{\Gamma(\sigma)} \sum_{y=0}^k f_{y,k+1} \{ \sigma T - P_6 R \}.$$

From (29) and (30) obtained;

$$dy_{K+1} = K^{\sigma+1} - (k - \sigma)(k + \sigma)^\sigma, \quad y = 0$$

$$(k - y + 2)^{\sigma+1} + (k - \sigma)^{\sigma+1} - 2(k - y + 1)^{\sigma+1}, \quad 1 \leq y \leq k$$

and $f_{y,k+1} = \frac{g^\sigma}{\sigma} \left[(k - y + 1)^\sigma (k - y)^\sigma \right], \quad 0 \leq y \leq k.$

3.9 Importance of using the fractional Adam-Bashforth Moulton method in obtaining the numerical solutions of the model

1. The fractional Adams-Bashforth-Moulton method requires just one extra function evaluation per step, while maintaining high-order accuracy.
2. This method provides built-in error control and is widely used in ODE solvers for integration.
3. With its extensive applications in fields such as engineering, chemistry, and medicine, this method serves as a powerful tool for numerically solving both partial and fractional-order differential equations.

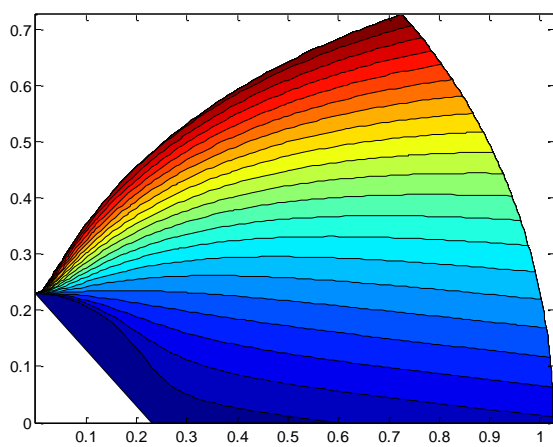


Fig. (1a): Contour plot showing the impact of β_1 and ω_1 on R_0

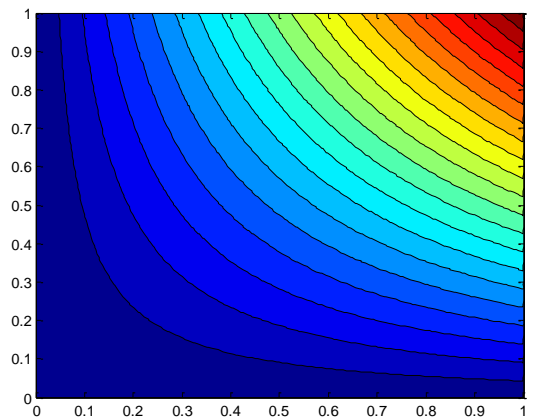
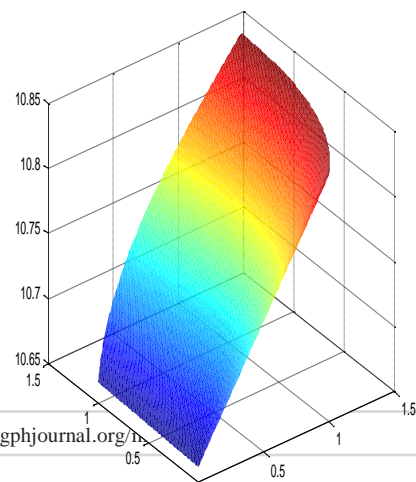
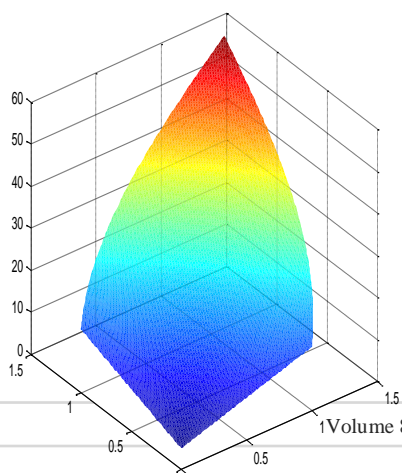


Fig. (1b): Contour plot showing the impact of α and ω_1 on R_0

(1a) shows the contour plot of concerning. A detailed examination of the numerical flow in the graph shows that the highest value of R_0 reached by modifying these parameters is 0.8, which is below one (1). This suggests that reducing β_1 and increasing ω_1 would not cause a substantial Chlamydia outbreak in the population.

(1b) The contour plot of concerning is shown. By examining the numerical flow within the graph, it is evident that the maximum value attained by adjusting these parameters is 0.8, which is below one (1). This indicates that increasing these parameters would not result in a major Chlamydia outbreak within the population.



(2a) It can be observed that the basic reproduction number reaches its highest point below one (1) as the values of β_1 reduces and the value of ω_1 increases. This indicates that reducing β_1 and increasing ω_1 will eventually reduce the impact of Chlamydia in the population. On the other hand, if necessary measures are not taken, β_1 can worsen the prevalence of Chlamydia. This is clear from their impact on R_0 .

(2b), It can be seen that the basic reproduction number peaks below one (1) as the values of ω_1 and α increases. This suggests that increasing these parameters will eventually reduce the impact of Chlamydia in the population. On the other hand, if proper measures are not taken, ω_1 and α can exacerbate the prevalence of chlamydia. This is clear from their influence on R_0 .

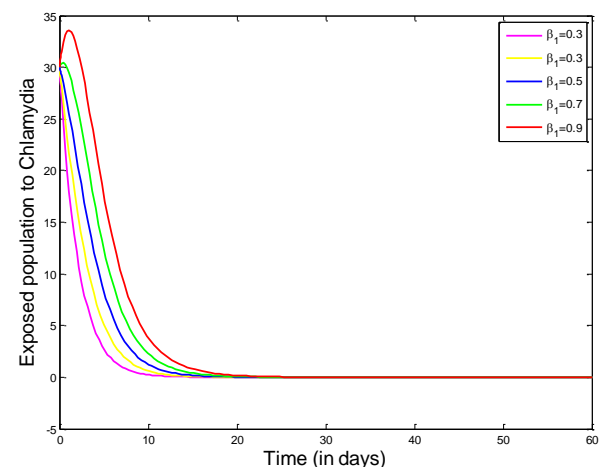
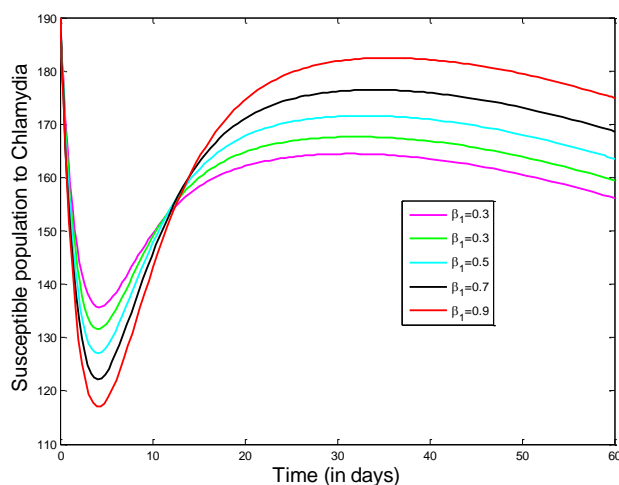
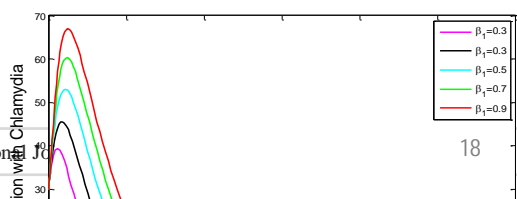
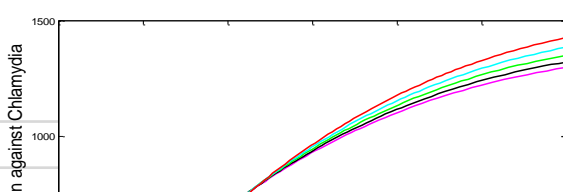


Fig. (3a): Susceptible population to Chlamydia

Fig. (3b): Exposed population to Chlamydia

(3a) illustrates the simulation of the impact of the contact rate (β_1) on Chlamydia in the susceptible population. It is observed that as the contact rate (β_1) rises, the number of susceptible individuals also increases. (3b) illustrates the simulation of the impact of the contact rate (β_1) on Chlamydia in the Exposed Human population. It is observed that, as the Contact rate (β_1) increases, the number exposed humans increases.



(3c) illustrates the simulation of the impact of the contact rate (β_1) on Vaccinated population against Chlamydia. It is observed that, as the Contact rate (β_1) increases, the number of Vaccinated populations against Chlamydia increases. (5c) illustrates the simulation of the impact of the contact rate (β_1) on Chlamydia in Infected population. It is observed that, as the Contact rate (β_1) increases, the number of infected populations increases.

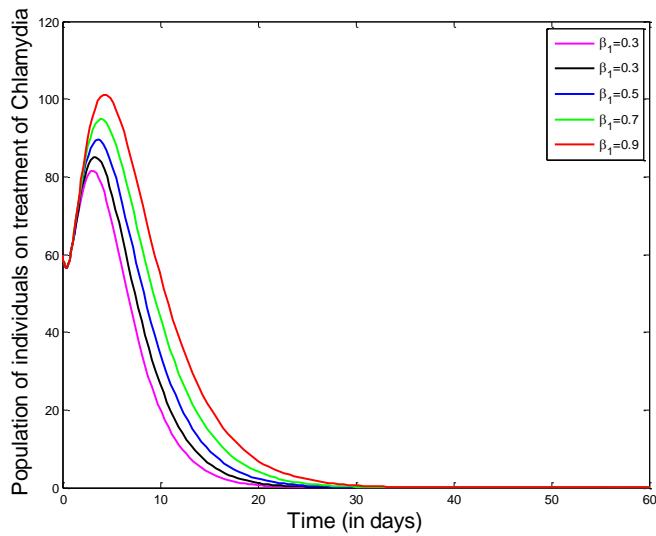


Fig. (3e): Population of individuals on treatment of Chlamydia

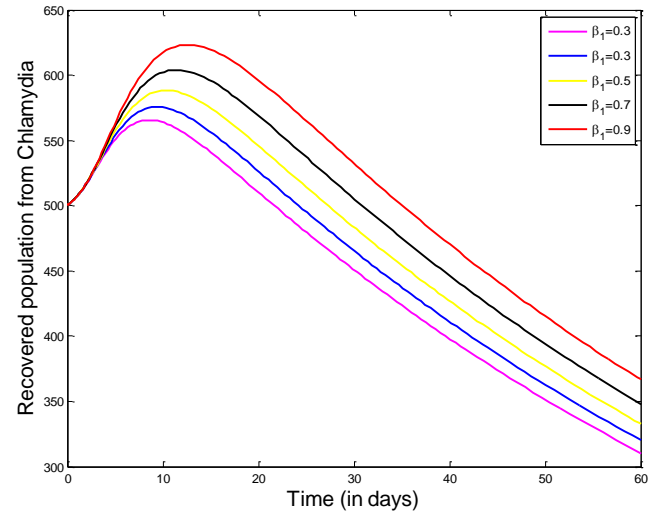
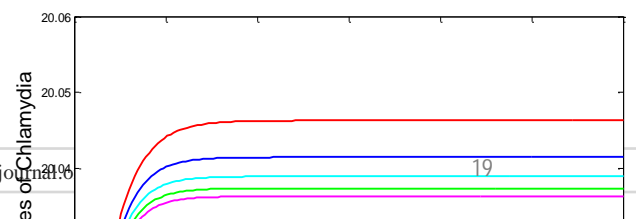
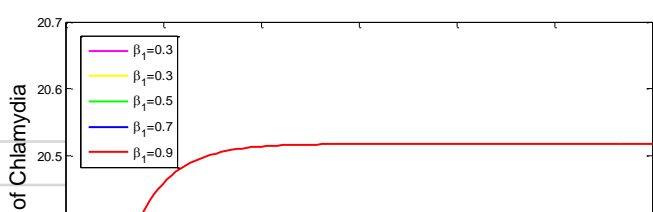


Fig. (3f): Recovered population from Chlamydia

(3e) illustrates the simulation of the impact of the contact rate (β_1) on Chlamydia on the Treatment population. It is observed that, as the Contact rate (β_1) increases, the number of humans in treatment class increases. (3f) illustrates the simulation of the impact of the contact rate (β_1) on Chlamydia on the Recovered population. It is observed that, as the Contact rate (β_1) increases, the number of Recovered populations' increases.



(3g) illustrates the simulation of the impact of the contact rate (β_1) on Chlamydia in the Cumulative new cases of Chlamydia. It is observed that, as the Contact rate (β_1) increases, the Cumulative new cases of Chlamydia increases. (3h) depicts the simulation of the effect of the treatment rate (α) on Chlamydia Cumulative new cases. It is noted that as the treatment rate (α) increases, the Cumulative new cases of Chlamydia decreases.

5.0 Conclusions

In this study, we propose a mathematical model to analyze the transmission dynamics and control strategies for Chlamydia, utilizing the Caputo fractional derivative. Recognizing the importance of fractional modeling, we conducted an in-depth theoretical analysis of the fractional Chlamydia model, emphasizing the existence and uniqueness of solutions as well as the stability of equilibrium points. For numerical solutions, we employed the fractional Adams–Bashforth–Moulton method. The simulations illustrated the influence of model parameters and varying fractional orders of the Caputo operator on disease incidence. Additionally, we examined the impact of modifying parameters such as the contact rate between infected and susceptible individuals and the treatment rate. The results suggest that enhancing treatment and vaccination efforts could substantially reduce the prevalence of Chlamydia in the population. Future studies could explore solving non-linear partial differential equations using symbolic computing techniques, such as those introduced by Zhang et al. [26], to obtain analytical solutions.

Data Availability

All data used in the course of this work are well cited in the work and referenced accordingly.

Conflict of interest

The authors declared no conflict of interest.

4.23 Parameter Values and Sources

Parameter	Value	Source
π	0.05	[27]
ϕ	0.3	[28]
ω_1	0.095	Estimated
ω_2	0.5	[29]
μ	0.01245	[29]
θ	0.7	[28]
α	0.2	[30]
β_1	0.096	Estimated
β_2	0.085	Estimated
δ_1	0.3	Estimated
δ_2	0.21	Estimated
σ	0.23	Estimated

6.0 References

- [1] Global prevalence and incidence of selected curable sexually transmitted infections: overview and estimates [Internet]. World Health Organization; c2001 [cited 2022 Feb 10]. Available from: <https://apps.who.int/iris/bitstream/handle/10665/66818/?sequence=1>
- [2] World Health Organization. Global progress report on HIV, viral hepatitis and sexually transmitted infections, 2021: accountability for the global health sector strategies 2016–2021: actions for impact: web annex 2: data methods. World Health Organization; 2021.
- [3] Thylefors B, Négrel AD, Pararajasegaram R, Dadzie KY. Global data on blindness. Bull World Health Organ. 1995; 73:115–21.
- [4] Newman L, Rowley J, Vander Hoorn S, Wijesooriya NS, Unemo M, Low N, et al. Global estimates of the prevalence and incidence of four curable sexually transmitted infections in 2012 based on systematic review and global reporting. PLoS One. 2015;10:e0143304.
- [5] Sexually transmitted infections (STIs) [Internet]. World Health Organization; c2021 [cited 2022 Feb 10]. Available from: [https://www.who.int/en/news-room/fact-sheets/detail/sexually-transmitted-infections-\(stis\)](https://www.who.int/en/news-room/fact-sheets/detail/sexually-transmitted-infections-(stis))
- [6] Chlamydia – CDC basic fact sheet [Internet]. USA: CDC; [cited 2022 Feb 10]. Available from: <https://www.cdc.gov/std/chlamydia/stdfact-chlamydia.htm>
- [7] Paavonen J, Lehtinen M. Chlamydial pelvic inflammatory disease. Hum Reprod Update. 1996; 2:519–29.
- [8] Paavonen J, Eggert-Kruse W. Chlamydia trachomatis: impact on human reproduction. Hum Reprod Update. 1999; 5:433–47.

- [9] Diethelm .K., (2022) The Frac PECE subroutine for the numerical solution of differential equations of fractional order, DOI: <https://doi.org/10.33003/fjs-2023-0706-2174>.
- [10] Podlubny.I., (1998) Fractional differential equations, an introduction to fractional derivatives, in: Fractional Differential Equations, to Methods of their Solutions and Some of their Applications, Elsevier.
- [11] Atokolo, W., Aja, R. O., Aniaku, S. E., Onah, I. S., & Mbah, G. C. (2022). Approximate solution of the fractional order sterile insect technology model via the Laplace– Adomian Decomposition Method for the spread of Zika virus disease. *International Journal of Mathematics and Mathematical Sciences*, 2022(1), 2297630.
- [12] Atokolo W a, Remigius Aja .O. , Omale .D., Ahman .Q. O., Acheneje G. O., Amos . J. (2024) Fractional mathematical model for the transmission dynamics and control of Lassa fever *Journal of journal homepage: www.elsevier. 2773-1863/© 2024com/locate/fraope* <https://doi.org/10.1016/j.fraope.2024.100110>.
- [13] Yunus. A.O, M.O. Olayiwola, M.A. Omolaye, A.O. Oladapo, (2023) A fractional order model of lassa fever disease using the Laplace-Adomian decomposition method, *Health Care Anal. 3* 100167, www.elsevier.com/locate/health. Health care Analytics.
- [14] Omede.B. I, Israel. M., Mustapha .M. K. , Amos J. , Atokolo .W. , and Oguntolu .F. A. (2024) Approximate solution to the fractional soil transmitted Helminth infection model using Laplace Adomian Decomposition Method. *Journal of mathematics. (2024) Int. J. Mathematics. 07(04), 16-40.*
- [15] Amos J., Omale D., Atokolo W., Abah E., Omede B.I., Acheneje G.O., Bolaji B. (2024), Fractional mathematical model for the Transmission Dynamics and control of Hepatitis C, *FUDMA Journal of Sciences*, Vol.8, No.5, pp.451-463, DOI: <https://doi.org/10.33003/fjs-2024-0805-2883>.
- [16] Philip J., Omale D., Atokolo W., Amos J., Acheneje G.O., Bolaji B. (2024), Fractional mathematical model for the Transmission Dynamics and control of HIV/AIDs, *FUDMA Journal of Sciences*, Vol.8, No.6, pp.451-463, DOI: <https://doi.org/10.33003/fjs-2024-0805-2883>.
- [17] Abah E., Bolaji B., Atokolo W., Amos J., Acheneje G.O., Omede B.I, Amos J., Omeje D. (2024), Fractional mathematical model for the Transmission Dynamics and control of Diphtheria , *International Journal of mathematical Analysis and Modelling*, Vol.7, ISSN:2682-5694.
- [18] Ahmed I., . Goufo E. F. D, Yusuf A., Kumam .P., Chaipanya P., and Nonlaopon K. (2021), “An epidemic prediction from analysis of a combined HIV-COVID-19 co-infection model via ABC fractional operator,” *Alexandria Engineering Journal*, vol. 60, no. 3, pp. 2979–2995.
- [19] Smith, J., Johnson, A.B., & Lee, C. (2023), "Modeling the coinfection dynamics of hepatitis C and COVID-19: A systematic review," *Journal of Epidemiology and Infection*, 151(7), pp. 1350–1365.
- [20] Ullah. A.Z. T. Abdeljawad, Z. Hammouch, K. Shah, A hybrid method for solving fuzzy Volterra integral equations of separable type kernels, *J. King Saud Univ. - Sci.* 33 (2020) <http://dx.doi.org/10.1016/j.jksus.2020.101246>.

- [21] Das, R., Patel, S., & Kumar, A. (2024), "Mathematical modeling of hepatitis C and COVID-19 coinfection in low- and middle-income countries: challenges and opportunities," *BMC Public Health*, 24(1), pp. 587.
- [22] Ali.Z., Zada.A.,Shah. K., Existence and stability analysis of three-point boundary value problem, *Int. J. Appl. Comput. Math.*3 (2017) 651–664, <http://dx.doi.org/10.1007/s40819-017-0375-8>.
- [23] Milici C., G. Draganescu, J.T. Machado, *Introduction to Fractional Differential Equations*, Springer, 2018.
- [24] Bonyah. E., Zarin, R. Fatmawati, Mathematical modeling of Cancer and Hepatitis co-dynamics with non-local and nonsingular kernel, 2020, 2052–2541.<https://doi.org/10.28919/cmbn/5029>.
- [25] Baskonus. H.M., Bulut H., (2015) On the numerical solutions of some fractional ordinary differential equations by fractional Adams Bashforth-Moulton Method, *Open Math.* 13 1.
- [26] Zhang.R.F.,Li. M.-C.,Gan. J.Y., Li.Q., Lan.Z.-Z., (2022). Novel trial functions and rogue waves of generalized breaking soliton equation via bilinear neural network method, *Chaos Solitons Fractals* 154 (C). *Results in Physics*, vol. 37, article 105498.
- [27] Nyarko Christiana Cynthia, Nsowa-Nuamah Nicholas Nicodemus Nana, Nyarko Peter Kwesi, Wiah Eric Neebo, Buabeng Albert Modelling Chlamydia trachomatis infection among Young women in Ghana: A case study at Tarkwa Nsuaem Municipality *Am. J. Appl. Math.*, 9 (3) (2021), pp. 75-85
- [28] Sharma Swarnali, Samanta G.P. Analysis of a Chlamydia epidemic model
J. Biol. Syst., 22 (04) (2014), pp. 713-744.
- [29] Odionyenma U.B., Omame A., Ukanwoke N.O., Nometal. Optimal control of Chlamydia model with vaccination *Int. J. Dyn. Control*, 10 (1) (2022), pp. 332-348.
- [30] Samanta G.P., Sharma Swarnali, Analysis of a delayed Chlamydia epidemic model with pulse vaccination *Appl. Math. Comput.*, 230 (2014), pp. 555-569.
- [31] Atokolo W a, Remigius Aja .O. , Omale .D., Paul .R. V. , Amos . J., Ocha S. O., (2023) Mathematical modeling of the spread of vector borne diseases with influence of vertical transmission and preventive strategies *FUDMA Journal of sciences*: Vol. 7 No. 6, December (Special Issue), pp 75-91 DOI: <https://doi.org/10.33003/fjs-2023-0706-2174>